



Contents lists available at ScienceDirect

Saudi Journal of Biological Sciences

journal homepage: [www.sciencedirect.com](http://www.sciencedirect.com)

Original article

# Fungicidal synergistic effect of biogenically synthesized zinc oxide and copper oxide nanoparticles against *Alternaria citri* causing citrus black rot disease



Momina Sardar<sup>a</sup>, Waqas Ahmed<sup>a</sup>, Samha Al Ayoubi<sup>b</sup>, Sobia Nisa<sup>a</sup>, Yamin Bibi<sup>c,\*</sup>, Maimoona Sabir<sup>a</sup>, Muhammad Mumtaz Khan<sup>a</sup>, Waseem Ahmed<sup>d</sup>, Abdul Qayyum<sup>e,\*</sup>

<sup>a</sup> Department of Microbiology, The University of Haripur, Haripur 22620, Pakistan

<sup>b</sup> Department of General Sciences, Prince Sultan University, Rafha Street, Riyadh, Saudi Arabia

<sup>c</sup> Department of Botany, PMAS-Arid Agriculture University Rawalpindi, Rawalpindi 46300, Pakistan

<sup>d</sup> Department of Horticulture, The University of Haripur, Haripur 22620, Pakistan

<sup>e</sup> Department of Agronomy, The University of Haripur, Haripur 22620, Pakistan

## ARTICLE INFO

## Article history:

Received 8 June 2021

Revised 19 July 2021

Accepted 19 August 2021

Available online 25 August 2021

## Keywords:

Citrus black rot

XRD

SEM

Scherrer equation

Zinc oxide nanoparticles

Copper oxide nanoparticles

## ABSTRACT

Citrus black rot disease being caused by *Alternaria citri* is a major disease of citrus plants with 30–35% economic loss annually. Fungicides had not been effective in the control of this disease during last few decades. In the present study, antifungal role of green synthesized zinc oxide (ZnO) and copper oxide (CuO) nanoparticles (NPs) were studied against *Alternaria citri*. *Alternaria citri* was isolated from disease fruits samples and was identified by staining with lacto phenol cotton blue. Furthermore, CuO and ZnO NPs were synthesized by utilizing the lemon peels extract as the reducing and capping agent. Nanoparticles were characterized by X-ray diffraction (XRD) and scanning electron microscopy (SEM) techniques. From the XRD data, the calculated size of CuO NPs was to be 18 nm and ZnO NPs was 16.8 nm using Scherrer equation. The SEM analyses revealed the surface morphology of all the metal oxide NPs synthesized were rounded, elongated and or spherical in the shape. The zone of inhibition was observed to be  $50 \pm 0.5$  mm by CuO NPs, followed by  $51.5 \pm 0.5$  mm by ZnO NPs and maximum zone of antifungal inhibition was observed to be  $53 \pm 0.6$  mm by mix metal oxide NPs. The results of minimum inhibitory concentration (MIC) and minimum fungicidal concentration (MFC) of the synthesized nanoparticles showed that at the certain concentrations ( $80 \text{ mg ml}^{-1}$ ), these NPs were capable of inhibiting the fungal growth, whereas above that specified concentrations ( $100 \text{ mg ml}^{-1}$ ), NPs completely inhibited the fungal growth. Based on these findings, the green synthesized NPs can be used as alternative to fungicide in order to control the citrus black rot disease.

© 2021 The Author(s). Published by Elsevier B.V. on behalf of King Saud University. This is an open access article under the CC BY-NC-ND license (<http://creativecommons.org/licenses/by-nc-nd/4.0/>).

## 1. Introduction

The production and development of nanomaterial by using copper, zinc, titanium, gold, magnesium, silver whose size ranges from 1 to 100 nm is known as nanotechnology (Hasan, 2015). Nanopar-

ticles are smaller than objects, but larger than atoms (Guisbiers et al., 2012). Nanoparticles are now being used in daily life requirement like in cosmetics, garment and different industries. Different methods are used for their synthesis involving biological, physical or chemical methods (Hasan, 2015). These NPs are used in different biological applications like treating diseases, preventing wound infection and having antimicrobial activities because of their smaller size (Duran et al., 2016).

Citrus Black rot is a major disease of citrus plant caused by a fungal plant pathogen *Alternaria citri*. It forms black hyphae on the surface of the plant and decline in citrus production. The disease prevails throughout the world leading to severe internal damage to citrus fruit and economic losses. In Pakistan, this disease accounts for 30–35% economic loss annually (Anwaar

\* Corresponding authors.

E-mail addresses: [dryaminbib@uaar.edu.pk](mailto:dryaminbib@uaar.edu.pk) (Y. Bibi), [aqayyum@uoh.edu.pk](mailto:aqayyum@uoh.edu.pk) (A. Qayyum).

Peer review under responsibility of King Saud University.



<https://doi.org/10.1016/j.sjbs.2021.08.067>

1319-562X/© 2021 The Author(s). Published by Elsevier B.V. on behalf of King Saud University.

This is an open access article under the CC BY-NC-ND license (<http://creativecommons.org/licenses/by-nc-nd/4.0/>).

et al., 2020). This is a disease of sweet oranges (*Citrus sinensis*) that occurs after harvesting the fruit. This disease prevails in extreme weather conditions like hot, dry summer, cool and moist winters. Citrus black rot begins as a core rot where pathogen colonizes the columella of the fruit. Citrus black rot disease may be caused by more than one morphological species of *Alternaria*, including species other than *Alternaria citri* (Mojerlou and Safaie, 2012). Initial route of the infection is only limited to the internal tissues. This results in the internal decay which causes the fruit to ripe prematurely. Citrus production decline is a global problem and is usually associated with poorly aerated soils. Leaves of the affected citrus trees may show symptoms related to zinc deficiency by the accumulation of zinc in bark and outer xylem of the trunk.

In a ten year survey of citrus associated diseases from several countries of the Mediterranean basin, high diseases pressure has been detected in all areas forcing citrus growers for adaptation of fungicidal spray programs. Chemical control leads to hazardous consequences for human and environmental health and, further, the widespread resistance phenomena limitize continuous applications of fungicides (Vitale et al., 2021). Thus, there is a need to hunt for new antifungal agents to control disease (Yang et al., 2019). Nanotechnology is an emerging technology with the potential application in plant protection. The use of NPs suggests a new promising approach to control fungal infections in plants. These little particles of matter possess unique antifungal properties and may be used as an alternative to fungicides (De la Rosa-García et al., 2018). Fungal infections in citrus can be controlled using alternative techniques. The combination therapy of Ag NPs along with fungicidal compound like epoxiconazole against *Setosphaeria turcica* fungi showed some promising results, indicating possible synergistic effect of NPs along with drugs (Huang et al., 2020). But no data is available to indicate antimicrobial efficacy of two or more metal oxide NPs and their combined effect against pathogenic fungi. Green synthesis of NPs is a cheap, eco-friendly method and requires no toxic chemicals with little or no side effects (Irvani et al., 2014). In present decade efforts have been diverted to develop potent, effective and multi-functional nano-materials. Combined NPs have been utilized for the development of pesticide exhibiting improved biological potential and better environmental safety (Alghuthaymi et al., 2021). Therefore, present study was aimed to green synthesize ZnO and CuO NPs in order to study their antifungal properties against citrus black rot causing *Alternaria citri*, alone and in combination. Findings of the study may lead to development of an alternative effective method to control phytopathogenic fungi as compared to harmful fungicides.

## 2. Material and methods

### 2.1. Sample collection

About 100 samples with visible symptoms of citrus black rot disease were collected from orchards of District Haripur, Khyber Pakhtunkhwa, Pakistan in sterile polyethylene bags and stored till further use.

### 2.2. Preparation of media

Potato dextrose agar media (CM0139; Oxoid) was prepared according to manufacture recommendations. In brief, 39 g of potato dextrose agar was suspended in one liter distilled water. Media was then autoclaved at 121 °C for 15 min to sterilize. It was cooled to 45–50 °C and then poured in sterile plates in uniform manner and allowed to solidify.

### 2.3. Isolation of fungus

Samples were washed with distilled water and dried under shade at the room temperature. The borderline between the healthy and infected tissues of the surface fruit were cut with the help of a sterile razor blade. The cut portions were disinfected with 70% ethanol for 2 min. The infected part showing lesions were placed in potato dextrose agar containing streptomycin (100 mg ml<sup>-1</sup>) to prevent the growth of bacteria. The inoculum was incubated at room temperature (28 °C) for 5 days (Parey et al., 2013).

### 2.4. Identification of fungus

A drop of lacto-phenol cotton blue was placed in the middle of clean glass slide. Few mycelia were placed on glass slide using inoculating wire loop. Teasing was done to separate the mycelium in order to get a homogenous mixture covered with coverslip and allowed to stay for few min. The presence of thread like hyphae, microconidia and club shaped black or brown spores were observed under the microscope.

### 2.5. Green synthesis of nanoparticles

#### 2.5.1. Copper oxide nanoparticles synthesis

Copper oxide nanoparticles were produced by following the green synthesis technique. Copper sulphate pentahydrate (CuSO<sub>4</sub>·5H<sub>2</sub>O) was utilized to form the CuO NPs by utilizing the lemon peels extract. Lemons were collected from the local market of Haripur and peels were separated. Peels were washed three times with the distilled water (dH<sub>2</sub>O) and kept for shade drying at room temperature for seven days. Dried peels were pulverized to fine powder using a sterilized mixer grinder and stored in air tight bottles.

200 ml distilled water was measured and placed in a conical flask and 10 g of copper sulphate pentahydrate was weighed and added to the heating distilled water. 15 g of prepared lemon peel extract was added drop wise to the CuSO<sub>4</sub> solution and change in color from blue to dark brown was noted. The prepared NPs solution was cooled and filtered using Whatman filter paper No 1. Filtered concentrated NPs solution was placed for drying in china dish in hot air-oven for 1 hr. Later the NPs were scratched from the surface of the china dish and grinded. Copper oxide NPs powder was dissolved in distilled water (dH<sub>2</sub>O) to prepare different concentrations of CuO NPs for further use.

#### 2.5.2. Zinc oxide nanoparticles synthesis

For preparation of ZnO NPs 10 g of zinc chloride was dissolved to 200 ml of hot distilled water. Then 15 g of the prepared lemon peel extract was drop wise added to the solution. The whole mixture was boiled for half hour and change in color was noted from rust to light brown. The prepared NPs solution was then placed for cooling. Later, the concentrated solution of the NPs was dried in china dish in hot air oven at 80 °C for 1 hr. After drying, the NPs were scratched from the surface of china dish and grinded. Further, the grinded ZnO NPs powder was weighed to prepare different concentrations in distilled water for further use.

### 2.6. Characterization of nanoparticles

The green synthesized ZnO and CuO NPs were characterized for their crystalline structure and morphology through XRD (X'pert PRO of PANalytical company), and SEM (JOEL-JSM-6490LA™ SEM) respectively. XRD carried out diffraction analysis at a wavelength (λ) of 1.5418 Å within a 2θ range of 10–80°. The morphology of the synthesized NPs was performed using SEM with a counting

rate of 2838 cps by SEM operating at 20 kV (Jamdagni et al., 2018; Geetha et al., 2016).

### 2.7. Antifungal activity of nanoparticles

About 39 g of potato dextrose agar (PDA) was measured and added to 100 ml distilled water and dissolved by proper stirring. After autoclaving, the media plates were placed for solidification for about 20–25 min. Wells were prepared in the solidified media using sterilized cork borer (8 mm). The wells were properly sealed with 20  $\mu$ l of media (that was placed in water bath to prevent from the solidification). After sealing the wells, the plates were then again placed to solidify for 10 min. Plates were then inoculated with 50  $\mu$ l of fungal culture. Next, about 100  $\mu$ l of NPs prepared in different concentration in distilled water were poured in the wells. The plates were then placed as such for about 40–45 min so that the NPs get disperse in the media properly. After 40–45 min, the plates were then placed in the incubator for 5 days at 28C. After 5 days, the plates were observed for the antifungal activity. The zones of inhibition were measured and recorded with respect to the type and concentration of the NPs with the help of scale to mm accuracy.

### 2.8. Minimum inhibitory concentration determination of nanoparticles

About 1.3 g of nutrient broth were measured and added to the conical flask that contained 100 ml of the distilled water. The nutrient broth was subjected to autoclaving at 121C for 20 min at 15 psi. After autoclaving, the nutrient broth was placed to cool down. After cooling, approximately 9 ml nutrient broth was taken from the flask and poured into the falcon tubes/screw-capped glass tubes. About 1 ml of the respective fungal strain was taken and added into this 9 ml broth along with different concentration of NPs in each tube. This tube was incubated in the shaker incubator for 24 h. After 24 h of incubation, the samples were observed visually. On the basis of visual observation, the MIC was determined at a certain concentration.

### 2.9. Evaluation of synergistic effect of mix metal oxide nanoparticles

The mix NPs were prepared after the drying of both the CuO and ZnO NPs. Dried powder of CuO NPs and ZnO NPs was weighed in equal amount and dissolved in distilled water to check their synergistic effect against *Alternaria citri*. The fractional inhibitory concentration (FIC) index was evaluated with modification (Dzotam et al., 2015). FIC value for each NP was calculated from MIC of NP showing no visible growth when used in combination.

FIC (CuO) = MIC of CuO in combination / MIC of CuO alone

FIC (ZnO) = MIC of ZnO in combination / MIC of ZnO alone

Synergistic effect  $0.5 \geq \sum \text{FIC}$

Indifferent effect  $0.5 < \sum \text{FIC} \leq 0.4$

Antagonism effect  $\sum \text{FIC} > 4$

### 2.10. Minimum fungicidal concentration determination of nanoparticles

About 39 g of PDA was measured and added to the conical flask that contained 100 ml of the distilled water. The agar was then autoclaved at 121C for 20 min at 15 psi. After autoclaving, media was placed at the room temperature for 10 min. Later, pouring of media was done in the sterilized Petri-plates. The plates were then let to solidify for about 20 min. After solidification, inoculating loop was dipped into the glass tubes to determine MFC and the sample was inoculated on the agar plates. The inoculated plates were incubated at 28C. The plates were then observed for minimum as well

as no visible growth. The selected concentrations with negative growth were declared as MFC.

### 2.11. Statistical analysis

Experiments were conducted in triplicate and average with standard deviation was calculated. Analysis of variance (ANOVA) was performed to test statistical significance of results between the groups. Graph Prism 9.1 version was used to perform ANOVA.

## 3. Results

### 3.1. Scanning electron microscopy analysis of zinc oxide nanoparticles

Surface morphology of the ZnO NPs was elucidated by using SEM (Fig. 1). Scanning electron microscopy images showed various morphological appearance of the ZnO NPs. Majority of the NPs were spherical in shape and some were elongated in shape. Some variations were noticed in the NPs size. The size of ZnO NPs ranged from 14.57 nm to the 49.88 nm and the mean size of the NPs were estimated to be 33.92 nm (Fig. 1).

### 3.2. Scanning electron microscopy analysis of copper oxide nanoparticles

The size and shape of the obtained CuO NPs were studied using SEM technique (Fig. 2). The NPs have good homogeneity, spherical in shape and appropriate separation. A homogenous distribution of particles gives us better knowledge on the particle size and approximately particle size. The size of the CuO NPs ranged from 18.18 nm to 43.37 nm with the mean size of the CuO NPs about 25 nm (Fig. 2).

### 3.3. X-Ray diffraction analysis of copper oxide nanoparticles

The XRD peaks of CuO NPs being synthesized by using lemon peel extract as a reducing agent has been described in Fig. 3. The resulting spectrum of CuO NPs appeared at 2-theta degree range of 36, 45, 65 and 77 for the respective indices of 11, 200, 220 and 311. These peaks can be characterized according to crystalline structures corresponding to the synthesis of pure CuO NPs. The crystalline nature of CuO NPs can be determined by observing the narrow sharp peaks. These peaks thus imply the high purity of synthesized CuO NPs that is achieved by following the green synthesis technique. The crystal size affects the broadening of peaks. The calculated average crystallite size by Scherrer equation ( $D = k\lambda/\beta\cos\theta$ ) was 18 nm for CuO NPs. It was thus clear that the

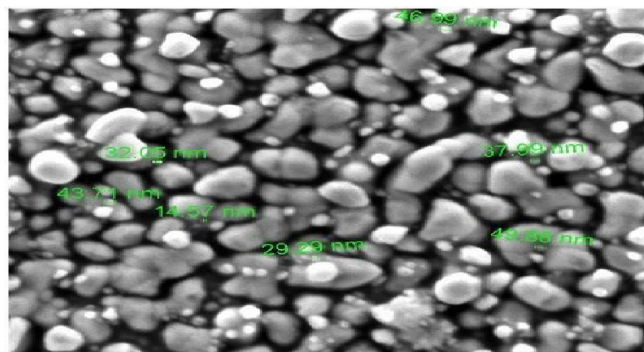


Fig. 1. Scanning electron microscopy (SEM) analysis of zinc oxide nanoparticles reveals nanoparticles size and shape.

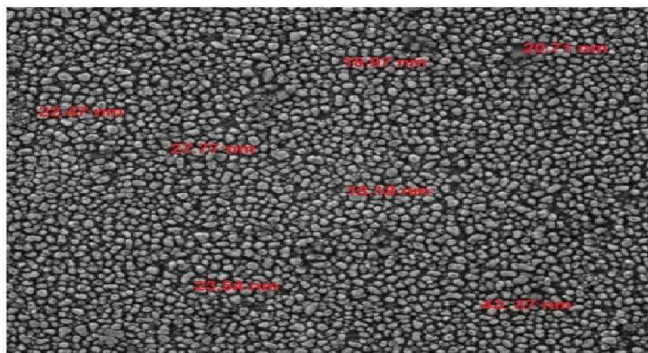


Fig. 2. Scanning electron microscopy (SEM) analysis of copper oxide nanoparticles reveals nanoparticles size and shape.

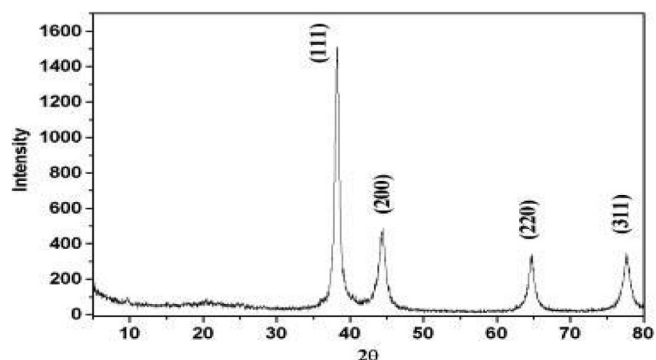


Fig. 3. X-ray diffraction (XRD) analysis of copper oxide nanoparticles.

pure CuO NPs have been synthesized by using copper sulfate as a precursor (Fig. 3).

### 3.4. X-ray diffraction analysis of zinc oxide nanoparticles

The XRD peaks of ZnO NPs synthesized using lemon peel extract for reducing zinc chloride have been shown in Fig. 4. The characteristic peaks of ZnO NPs were observed at 2-theta range of 37°, 45°, 65°, 77° and 83° for the respective indices of 111, 200, 220, 311 and 222 respectively. The presence of sharp peaks has indicated that the ZnO NPs synthesized were highly pure and free from contamination. The narrowing of XRD peak was thought to be affected by the crystal size. The average crystallite size calculated by Scherrer equation ( $D = k\lambda/\beta\cos\theta$ ) was 16.8 nm. It was observed that pure ZnO NPs have been synthesized via using zinc chloride as a precursor (Fig. 4).

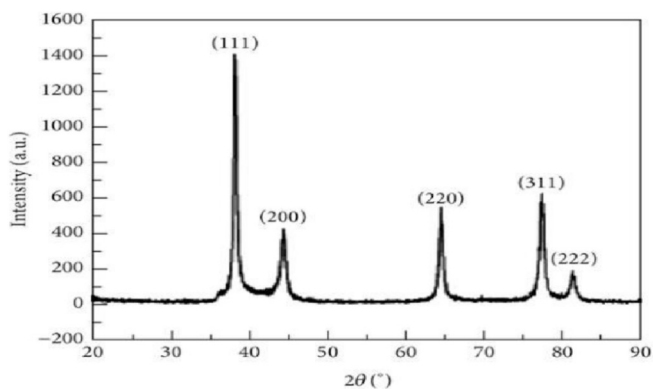


Fig. 4. X-ray diffraction (XRD) analysis of zinc oxide nanoparticles.

### 3.5. Microscopy of fungal culture

The obtained fungus (*Alternaria citri*) appeared in the form of thread like hyphae with microconidia and club shaped black or brown spores. The spores were present singly or in the form of long chains (Fig. 5).

### 3.6. Evaluation of antifungal activity of nanoparticles

#### 3.6.1. Antifungal activity of zinc oxide nanoparticles

Antifungal activity of ZnO NPs synthesized by using lemon peel extract against *Alternaria citri* showed variable level of susceptibility at the various concentrations. Different concentrations of ZnO NPs were prepared ranging from 10 mg ml<sup>-1</sup> to 100 mg ml<sup>-1</sup> to assess the effectiveness of ZnO NPs against the selected *Alternaria citri* fungal strain (Fig. 6). At a concentration of 10 mg ml<sup>-1</sup> a zone of inhibition with 21.5 ± 0.5 mm diameter was observed. At 20 mg ml<sup>-1</sup> and 30 mg ml<sup>-1</sup>, the zone of inhibition was found to be 25 ± 0.5 mm and 26.5 ± 0.28 mm, respectively. A dose dependent response was found in the zone of the inhibition by increasing NPs concentration (Fig. 7). At various concentrations ranging from 40 mg ml<sup>-1</sup> to 90 mg ml<sup>-1</sup> different zone diameters ranging from 33.5 ± 0.05 mm to 46.5 ± 1.0 mm were documented. Highest zone of inhibition was recorded as 51.5 ± 0.5 mm at a concentration of 100 mg ml<sup>-1</sup>.

#### 3.6.2. Antifungal activity of copper oxide nanoparticles

Antifungal activity of green synthesized CuO NPs also exhibited varied level of antifungal activity against *Alternaria citri* (Fig. 8). At different concentrations ranging from 10 mg ml<sup>-1</sup> to 100 mg ml<sup>-1</sup> zones of clearance of varied diameter ranging from 18.5 ± 1 mm to 50 ± 0.5 mm were observed. Results indicated a dose dependent response that is by increasing the concentration of NPs the fungicidal effect was also enhanced (Fig. 9).

#### 3.6.3. Antifungal activity of mix metal oxide nanoparticles

The combined effect of the mix nanoparticles including both CuO and ZnO NPs was also determined against pathogenic fungi (*Alternaria citri*). Mix NPs were processed in the form of different dilutions ranging from 10 mg ml<sup>-1</sup> to 100 mg ml<sup>-1</sup> (Fig. 10). Zones of clearance of varied diameters ranging from 25 ± 0.2 mm to 53 ± 0.6 mm were observed at different concentrations of NPs (Fig. 11).

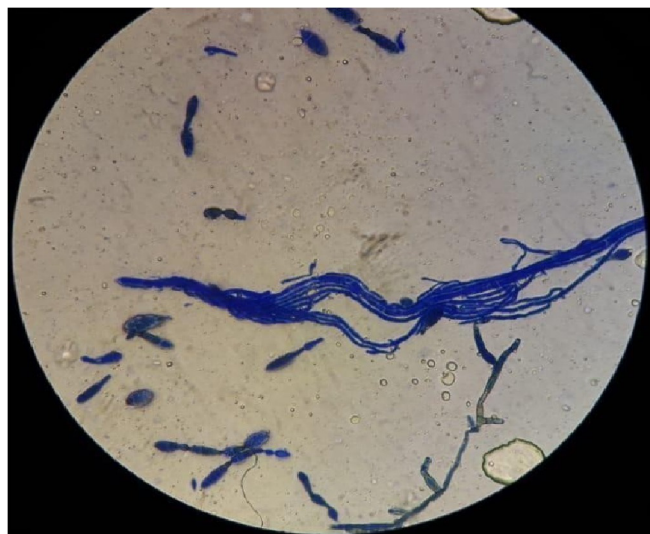
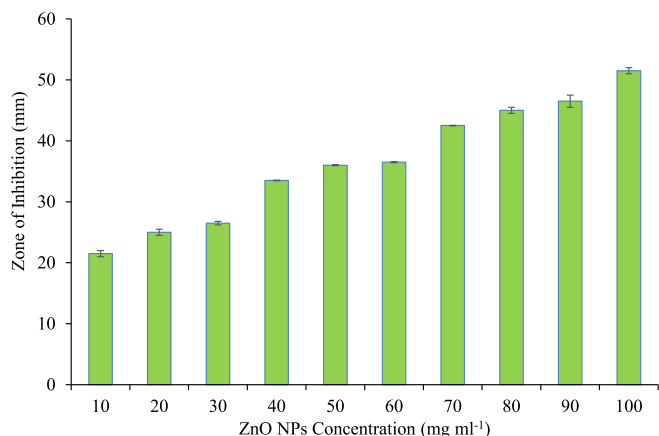


Fig. 5. Microscopic analysis of *Alternaria citri* showing typical hyphae of fungi.



**Fig. 6.** Inhibition zone (mm) recorded for antifungal effect of zinc oxide nanoparticles (n = 10).

### 3.7. Minimum inhibitory concentration and minimum fungicidal concentration determination of metal oxide nanoparticles

Following the MIC, MFC experiment, the synthesized CuO, ZnO and mix metal NPs exhibited the variable range of fungal growth inhibition. The MIC in case of CuO NPs synthesized by using lemon peel extract was 90 mg ml<sup>-1</sup>, while the MFC value of CuO NPs for *Alternaria citri* was 100 mg ml<sup>-1</sup> (Fig. 12). The MIC and MFC of ZnO NPs was also assessed by following the standard procedure. The MIC determined for *Alternaria citri* in case of ZnO NPs based on the use of lemon peel extract was 80 mg ml<sup>-1</sup> whereas the MFC value was 100 mg ml<sup>-1</sup> (Fig. 12). The MIC and MFC was also

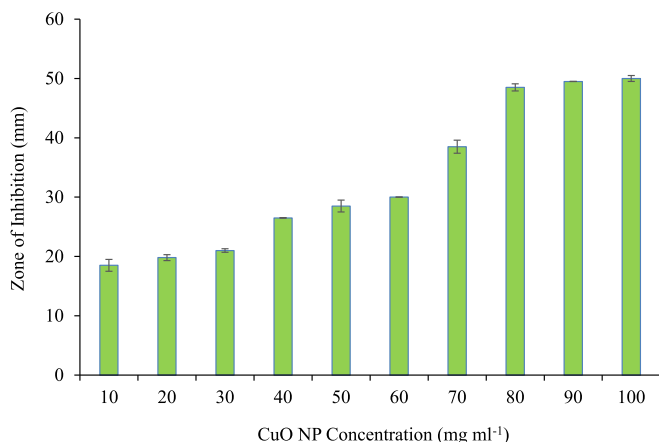


**Fig. 8.** Inhibition zone (mm) recorded for antifungal effect of copper oxide nanoparticles (n = 10).

assessed for the mix metal oxide NPs constituted on both CuO and ZnO NPs. Concerning the mix NPs the MIC and MFC was tested for *Alternaria citri*. The MIC value for *Alternaria citri* was 90 mg ml<sup>-1</sup>, while the MFC value was 100 mg ml<sup>-1</sup> (Fig. 12).

### 3.8. Evaluation of synergistic antifungal effect of nanoparticles

In order to find the combined antifungal effect of the synthesized NPs against *Alternaria citri*, fractional inhibitory concentration (FIC) was determined. The degree of combined effect of mixed NPs showed synergistic effect ( $\sum FIC = 0.3$ ) of both NPs when used in combination against the pathogenic fungi.

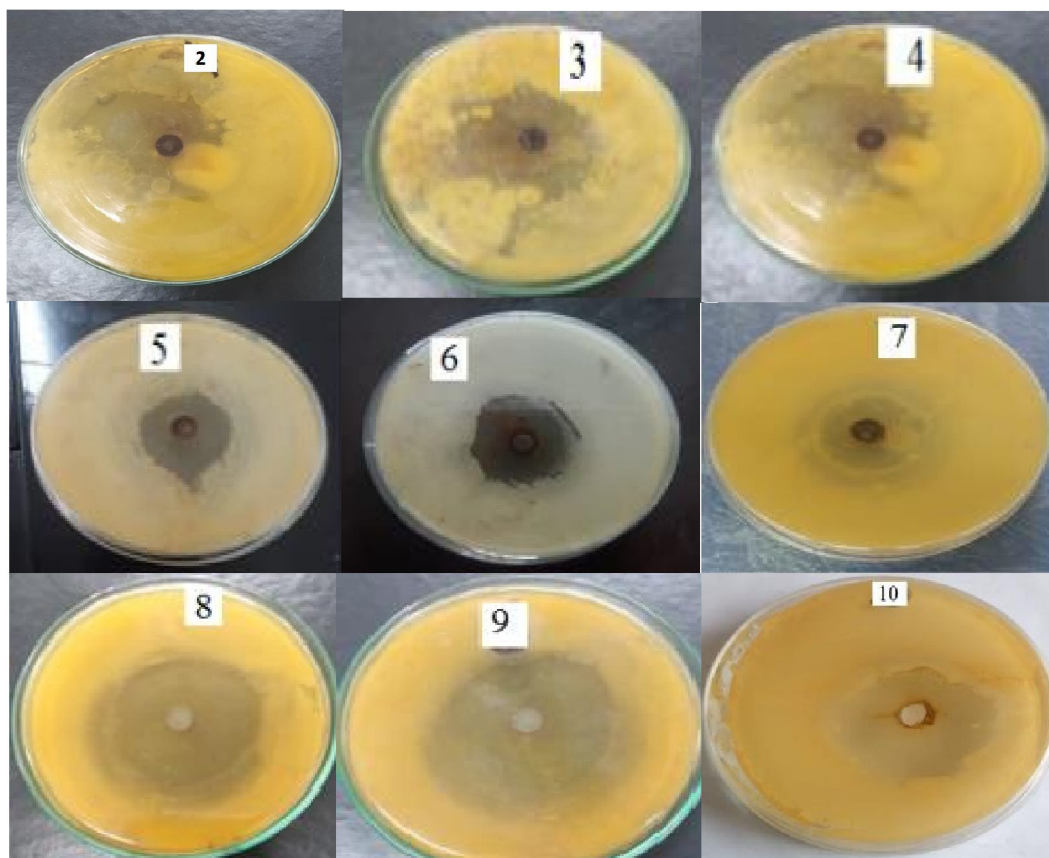


**Fig. 7.** Antifungal activity of zinc oxide nanoparticles showing zones of inhibition.

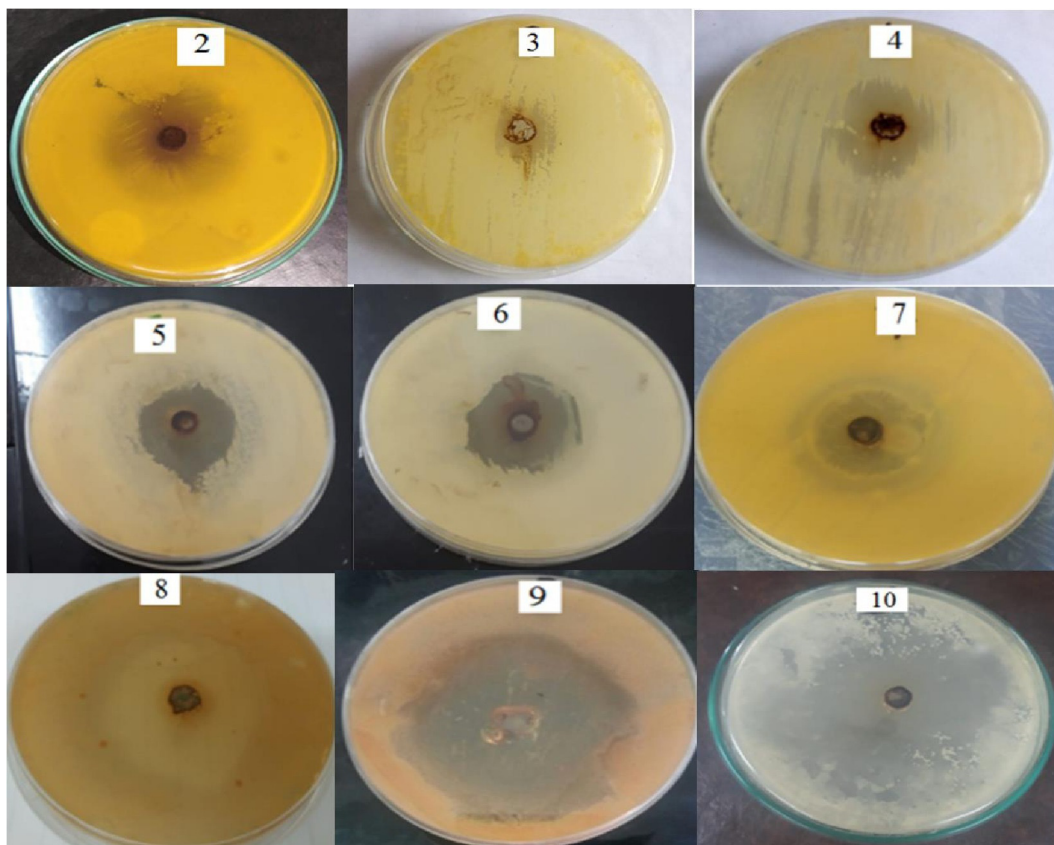


Fig. 9. Antifungal activity of copper oxide nanoparticles showing zones of inhibition.

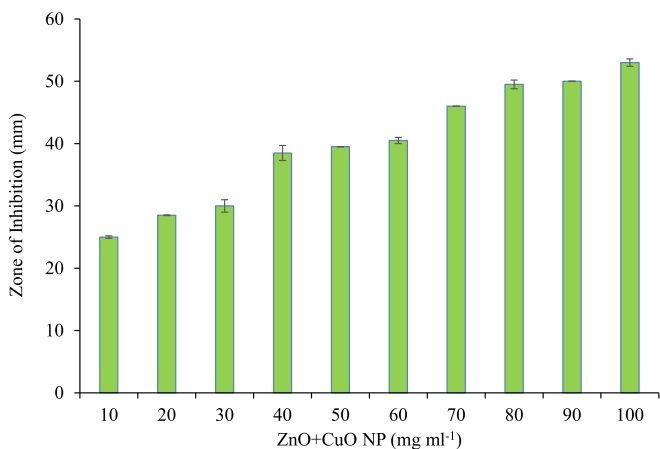


Fig. 10. Combined antifungal effects (Zones of clearance in mm) of zinc oxide and copper oxide nanoparticles on fungal growth.

#### 4. Discussion

Citrus black rot is major fungal disease of sweet oranges (*Citrus sinensis*) that affect the fruit even after post harvesting, leading to devastating impact on the overall production of oranges. *Alternaria citri* being prime etiological of the disease have been reported to develop fungicide resistance in last decade (Yang et al., 2019). Hence there is a need to use alternative techniques to control fungal infections. Nanoparticles can be used as an alternative to control phytopathogens in comparison to fungicides. Zinc oxide nanoparticles have wider applications and generally recognized

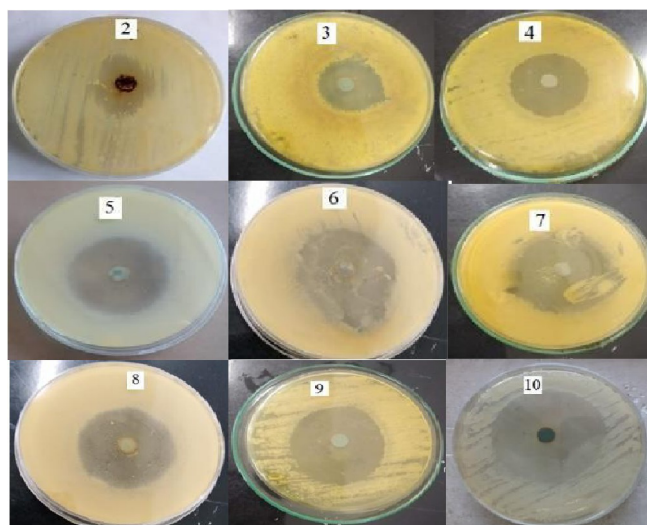
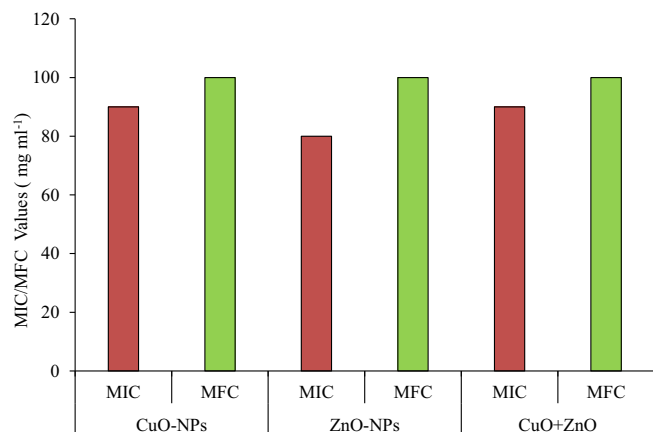


Fig. 11. Synergistic antifungal effects of zinc oxide and copper oxide nanoparticles 20–100 mg ml<sup>-1</sup> concentrations respectively.

as safe material by the US Food and Drug Administration (FDA, 2015) and ZnO NPs have increased applications in day-to-day lives including cosmetics ointments and food packaging etc. (Espitia et al., 2012; Marcous et al., 2017a; Marcous et al., 2017b). Zinc oxide has excellent photocatalytic activity and hence many applications (Rokhsat and Akhavan, 2016). Copper nanoparticles have received more attention in recent years as they are much cheaper than that of silver or gold nanoparticles thus their antifungal applications can be utilized in agriculture (Cao et al., 2014). Present



**Fig. 12.** Minimum inhibitory concentration (MIC) and minimum fungicidal concentration (MFC) determination of metal oxide nanoparticles against pathogenic fungi.

investigation revealed that green synthesis of CuO and ZnO NPs is very simple, safe and economic. Based on XRD analysis, the calculated sizes of ZnO and CuO NPs were 18 nm and 16.8 nm, respectively. These findings are supported by Sardella et al. (2017), who reported chemically synthesized ZnO NPs in size < 50 nm with antifungal activity against *Alternaria alternata* at 6 mM concentration in sweet oranges. Similarly, Youssef et al. (2017) reported antifungal effects of chemically synthesized Cu NPs having size of 45–48 nm against related fungi *Fusarium solani* in citrus fruit. Fungal surface is negatively charged at biological pH as a result of carboxyl and phosphate groups arrangements on the cell walls. Hence, positive charged ZnO NPs can make close physical interaction with fungi cells and can result in cell membrane damage and interaction with internal organelles (Espitia et al., 2012). Concerning the antifungal effect of the CuO, ZnO and mix metal oxide NPs, the combined / synergistic NPs including both CuO and ZnO NPs showed best antifungal activity of  $53 \pm 0.6$  mm at  $100 \text{ mg ml}^{-1}$  as compared to ZnO ( $51.5 \pm 0.5$  mm) and CuO ( $50 \pm 0.5$  mm) NPs alone. The results of MIC / MFC of the synthesized NPs showed that these NPs were found to be capable of inhibiting the fungal growth ( $80 \text{ mg ml}^{-1}$ ), whereas above that specified concentration NPs completely stop the fungal growth ( $100 \text{ mg ml}^{-1}$ ). A similar study was conducted by Al-Dhabaan et al. (2017) where Cu, ZnO NPs and copper nanocomposites were evaluated against phytopathogenic fungi; *Alternaria alternata*, *Rhizoctonia solani* and *Botrytis cinerea* to determine synergistic effects. The results demonstrated that nanocomposite exhibited higher activity at a concentration of  $90 \mu\text{g ml}^{-1}$ . Similarly antifungal activities of bimetallic blends at concentrations of 30, 60,  $90 \mu\text{g ml}^{-1}$  were effective to control growth of *Rhizoctonia solani*. Similarly, they demonstrated effective control of cotton seedling damping-off under greenhouse conditions (Abd-ElSalam et al., 2018). There are tremendous opportunities for application of green synthesized inorganic metal / metal oxide NPs in agriculture, particularly for the controlling and managing plant diseases caused by fungal pathogens. The nanomaterials should be tested for biocompatibility and toxic effects on non-target organisms for their proper applications (Saratale et al., 2018).

## 5. Conclusion

Citrus black rot disease, being one of major post-harvest disease of sweet oranges, has drastic impact on overall production of citrus fruit world-wide. Fungicidal resistance by the pathogen of this disease urges to find new possible alternative treatment. Nanoparti-

cles were reported to have good antifungal effect since long time. But chemical synthesis of metal oxide nanoparticles poses number of issues including production of toxic chemical gases during synthesis. Green synthesis of zinc and copper oxide nanoparticles using lemon peel extract has shown remarkable antifungal effect against *Alternaria citri* causing citrus black rot disease. The application of this environment friendly procedure of green synthesized metal oxide nanoparticles may help to reduce fungal infection in sweet oranges and improve the socioeconomic status of farmers as well.

## Declaration of Competing Interest

The authors declare that they have no known competing financial interests or personal relationships that could have appeared to influence the work reported in this paper.

## Acknowledgement

The authors would like to acknowledge the support of Prince Sultan University for paying the Article Processing Charges of this publication.

## References

- Abd-ElSalam, K.A., Vasil'kov, A.Y., Said-Galiev, E.E., Rubina, M.S., Khokhlov, A.R., Naumkin, A.V., Shtykova, E.V., Alghuthaymi, M.A., 2018. Bimetallic blends and chitosan nanocomposites: Novel antifungal agents against cotton seedling damping-off. *Eur. J. Plant Pathol.* 151, 57–72.
- Al-Dhabaan, F.A., Shoala, T., Ali, A.A.M., Alaa, M., Abd-ElSalam, K., 2017. Chemically-produced copper, zinc nanoparticles and chitosan-bimetallic nanocomposites and their antifungal activity against three phytopathogenic fungi. *Int. J. Agric. Technol.* 13, 753–769.
- Alghuthaymi, M.A., Rajkuberan, C., Rajiv, P., Kalia, A., Bhardwaj, K., Bhardwaj, P., Abd-ElSalam, K.A., Valis, M., Kuca, K., 2021. Nanohybrid antifungals for control of plant diseases: Current status and future perspectives. *J. Fungi* 7, 48. <https://doi.org/10.3390/jof7010048>.
- Anwaar, H., Iqbal, Z., Rehman, M.A., Mubeen, M., Abbas, A., Usman, H.M., Farhan, M., Sohail, M.A., Kiptoo, J.J., Iqbal, S., Moosa, A., Sajjad, K., 2020. Evaluation of fungicides and biopesticides for the control of *Alternaria black rot* disease in citrus. *Plant Cell Biotechnol. Mol. Biol.* 21 (33&34), 118–126.
- Cao, V.D., Nguyen, P.P., Khuong, V.Q., Nguyen, C.K., Nguyen, X.C., Dang, C.H., Tran, N. Q., 2014. Ultrafine copper nanoparticles exhibiting a powerful antifungal/killing activity against *Corticium salmonicolor*. *B Korean Chem. Soc.* 35 (9), 2645–2648.
- De la Rosa-García, S.C., Martínez-Torres, P., Gómez-Cornelio, S., Corral-Aguado, M.A., Quintana, P., Gómez-Ortiz, N.M., 2018. Antifungal activity of ZnO and MgO nanomaterials and their mixtures against *Colletotrichum gloeosporioides* strains from tropical fruit. *J. NanoMater.* <https://doi.org/10.1155/2018/3498527>.
- Duran, N., Durán, M., de Jesus, M.B., Seabra, A.B., Fávoro, W.J., Nakazato, G., 2016. Silver nanoparticles; A new view on mechanistic aspects on antimicrobial activity. *Nanomedicine.* 12 (3), 789–799.
- Dzotam, Singh, N.B., Brar, A., Singh, H., Singh, S.C., 2015. Antifungal activity and antifungal FIC indices of zinc oxide nanoparticles in combination with carbendazim, mancozeb and thiram. *Biotechnol. Lett.* 38 (4), 545–560.
- Espitia, P.J.P., Soares, N.D.F.F., Coimbra, J.S.D.R., de Andrade, N.J., Cruz, R.S., Medeiros, E.A.A., 2012. Zinc oxide nanoparticles: synthesis, antimicrobial activity and food packaging applications. *Food Bioprocess. Tech.* 5, 1447–1464.
- FDA, 2015. Select committee on GRAS substances opinion: Zinc salts. USA. <http://www.fda.gov/Food/IngredientsPackagingLabeling/GR>
- Geetha, M.S., Nagabhushana, H., Shivananjaiiah, H.N., 2016. Green mediated synthesis and characterization of ZnO nanoparticles using *Euphorbia jatropha* latex as reducing agent. *J. Sci-Adv. Mater. Dev.* 1 (3), 301–310.
- Guisbiers, Grégory, Mejía-Rosales, Sergio, Leonard Deepak, Francis, 2012. Nanomaterial properties: Size and shape dependencies. *J. Nanomater.* 2012, 1–2. <https://doi.org/10.1155/2012/180976>.
- Hasan, S., 2015. A review on nanoparticles; their synthesis and types. *Res. J. Recent Sci.* 4, 1–3.
- Huang, W., Yang, M., Duan, H., Bi, Y., Cheng, X., Yu, H., 2020. Synergistic antifungal activity of green synthesized silver nanoparticles and epiconazole against *Setospora turcica*. *J. Nanomater.* <https://doi.org/10.1155/2020/9535432>.
- Iravani, S., Korbekandi, H., Mirmohammadi, S.V., Zolfaghari, B., 2014. Synthesis of silver nanoparticles: chemical, physical and biological methods. *Res. Pharm. Sci.* 9 (6), 385–406.
- Jamdnagi, P., Khatir, P., Rana, J.S., 2018. Green synthesis of zinc oxide nanoparticles using flower extract of *Nyctanthes arbor-tristis* and their antifungal activity. *J. King Saud Univ. Sci.* 30 (2), 168–175. <https://doi.org/10.1016/j.jksus.2016.10.002>.

- Marcous, A., Rasouli, S., Ardestani, F., 2017a. Inhibition of *Staphylococcus aureus* growth in fresh calf minced meat using low density polyethylene films package promoted by titanium dioxide and zinc oxide nanoparticles. *J. Partic. Sci. Technol.* 3, 1–11.
- Marcous, Arin, Rasouli, Susan, Ardestani, Fatemeh, 2017b. Low-density polyethylene films loaded by titanium dioxide and zinc oxide nanoparticles as a new active packaging system against *Escherichia coli* O157:H7 in fresh calf minced meat. *Packag. Technol. Sci.* 30 (11), 693–701.
- Mojerlou, S., Safaie, N., 2012. Phylogenetic analysis of *Alternaria* species associated with citrus black rot in Iran. *J. Plant Pathol. Microb.* 3 (7), 144. <https://doi.org/10.4172/2157-7471.1000144>.
- Parey, M.A., Razdan, V.K., Sofi, T.A., 2013. Comparative study of different fungi associated with fruit rot of chilli and screening of chilli germplasm against *Colletotrichum capsici*. *Intl. J. Agri. Crop. Sci.* 5 (7), 723–730.
- Rokhsat, Eliza, Akhavan, Omid, 2016. Improving the photocatalytic activity of graphene oxide/ZnO nanorod films by UV irradiation. *Appl. Surf. Sci.* 371, 590–595.
- Saratale, Rijuta Ganesh, Karuppusamy, Indira, Saratale, Ganesh Dattatraya, Pugazhendhi, Arivalagan, Kumar, Gopalakrishanan, Park, Yooheon, Ghodake, Gajanan S., Bharagava, Ram Naresh, Banu, J. Rajesh, Shin, Han Seung, 2018. A comprehensive review on green nanomaterials using biological systems: Recent perception and their future applications. *Colloid. Surface B.* 170, 20–35.
- Sardella, Davide, Gatt, Ruben, Valdramidis, Vasilis P., 2017. Physiological effects and mode of action of ZnO nanoparticles against post-harvest fungal contaminants. *Food Res. Int.* 101, 274–279.
- Vitale, A., Aiello, D., Azzaro, A., Guarnaccia, V., Polizzi, G., 2021. An eleven-year survey on field disease susceptibility of citrus accessions to *Colletotrichum* and *Alternaria* species. *Agriculture* 11, 536. <https://doi.org/10.3390/agriculture11060536>.
- Yang, L.N., He, M.H., Ouyang, H.B., Zhu, W., Pan, Z.C., Sui, Q.J., Shang, L.P., Zhan, J., 2019. Cross-resistance of the pathogenic fungus *Alternaria alternata* to fungicides with different modes of action. *BMC Microbiol.* 19, 205. <https://doi.org/10.1186/s12866-019-1574-8>.
- Youssef, K., Hashim, A.F., Margarita, R., Alghuthaymi, M.A., Abd-Elsalam, K.A., 2017. Antifungal efficacy of chemically-produced copper nanoparticles against *Penicillium digitatum* and *Fusarium solani* on citrus fruit. *Philip. Agric. Sci.* 100, 69–77.